TECHNICAL UNIVERSITY OF CLUJ-NAPOCA

ACTA TECHNICA NAPOCENSIS

Series: Applied Mathematics, Mechanics, and Engineering

Vol. 68, Issue II, June, 2025

STRUCTURAL ANALYSIS OF THE DYNAMIC MODULAR FACADES PROCESSED BY U BENDING TECHNOLOGY

Cristina TEISANU, Nicoleta CIOATERA, Leonard Marius CIUREZU-GHERGHE, Gabriela SIMA, Cristian CHIHAIA, Cosmin MIRITOIU

Abstract: *Aluminium alloy EN AW-5754 is of particular interest to designers in the field of smart building facades, being capable of kinematic and dynamic architectural adjustments depending on the excessive operating climatic conditions (temperature, brightness, air flow). The study aims to carry out a complex structural analysis of facade modules from the alloy EN AW-5754, manufactured by U bending technology. To facilitate the volumetric displacement of the material during plastic deformation, respectively to avoid specific structural defects, the facade modules are accurately perforated along the curved bending lines; the laser beam technology allows different customized slot patterns for this purpose. The results of the analysis highlight the influence of the slots on the surface quality of the modules in the bending areas.*

Keywords: *building facades, cold forming, slot perforation, undulation surface, strain localisation*

1. INTRODUCTION

Dynamic facades are innovative building elements that enhance energy efficiency and occupant comfort by adapting to changing environmental conditions [1]. Utilizing advanced technologies and materials, these facades respond to light, temperature, wind and humidity, optimizing natural light and ventilation, and reducing the need for artificial lighting and HVAC systems (Heating, Ventilation and Air Conditioning) [2, 3]. They protect against extreme weather, modulate sunlight, reduce glare and control solar heat gain while maintaining a visually appealing design. Incorporating smart glass, movable shading devices and responsive insulation, dynamic facades provide consistent performance and resilience, contributing to healthier indoor environments. Overall, they represent a significant advancement in sustainable building design, balancing functionality, energy conservation and aesthetics.

Dynamic facades use advanced materials to adapt to environmental changes and enhance building performance: smart glass, Phase Change Materials, Photovoltaic Panels, Responsive Insulation Materials, and lightweight and durable ethylene tetrafluoroethylene (ETFE) foils. Also, Movable Shading Devices (MSD) as well as Perforated Metal Panels (PMP) control sunlight and ventilation, allowing air and light to pass through while reducing glare and heat gain, simultaneously providing insulation and light diffusion [4, 5].

Aluminium alloys are widely used in dynamic facades due to their exceptional properties and versatility. Being significantly lighter than other metals, they reduce the overall structural load and enable more innovative and flexible design options. Additionally, aluminium alloys offer high resistance to corrosion and weathering, making them ideal for exterior applications exposed to harsh environmental conditions. Despite their lightweight nature, aluminium alloys have excellent strength-to-weight ratios, ensuring structural stability and support for dynamic façade elements [6, 7]. Their good thermal conductivity can be managed with breaks to enhance energy efficiency in building facades. Aluminium alloys can be easily extruded, cast and formed into complex shapes, allowing for the creation of intricate and functional designs [8, 9, 10].

Received: 07.04.25; **Similarities**: 29.05.25: **Reviewed**: 07.04./ 07.04.25: **Accepted**:17.06.25.

Highly recyclable, aluminium alloys support sustainable building practices by reducing environmental impact. Various finishing methods such as anodizing, powder coating and painting can be applied to aluminium alloys to achieve desired aesthetics and durability. These attributes make aluminium alloys an ideal choice for dynamic facades, providing a balance of functionality, durability and design flexibility.

This work focused on the MSD and PMP as key components for dynamic facades, specifically on designing and manufacturing a metallic module at the lab scale that meets the aforementioned requirements. In this research, the aluminium alloy EN AW-5754 was used, as it is highly recommended for this application.

2. MATERIALS AND EXPERIMENTAL PROCEDURE

In the current work, 4 mm thickness commercial EN AW-5754 aluminium alloy sheets supplied by Vimetco Alro Slatina, Romania, were used to process the modular elements as the components for the dynamic facades (Fig. 1).

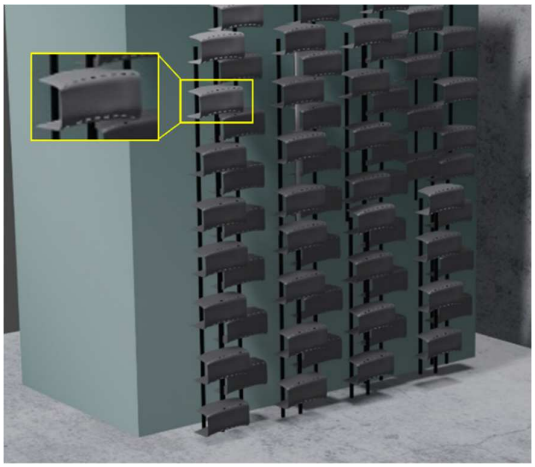

Fig. 1. Building dynamic façade – rendering image, focusing on the modular component

The chemical composition according to the manufacturer's quality certificate is: 2,9% Mg, 0,16% Mn, 0,37% Fe, 0,26% Si, 0,07% Cu, 0,02% Cr, 0,14% Zn, 0,01% Ni, max. 0,15% residuals and the rest is aluminium.

The mechanical properties of the aluminium alloy EN AW-5754 sheet were evaluated as per standard methods of tensile testing ASTM E8/E8M. The tensile test was performed at room temperature using an INSTRON 1000HDX universal testing machine with the maximum load of 1000 kN. The tensile specimens were tested along the rolling direction (RD - 0°), transversal direction (TD - 90°) and diagonal direction (DD - 45° between RD and TD), as shown in Figure 2. For each condition, five specimens were tested at a constant strain rate of 0,015 mm/mm/min and the true stress-strain curves were automatically recorded by the computer.

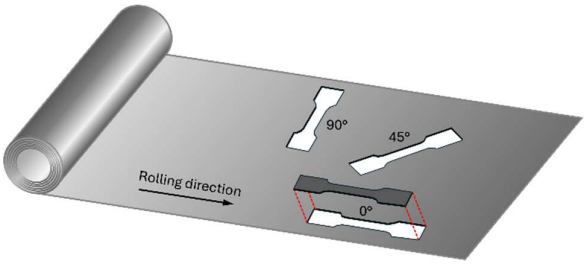

Fig. 2. The orientation of the samples for the tensile tests

The aluminium alloy sheets were cut into rectangular blanks of 100 mm x 140 mm for further processing through cold forming. The rectangular sheet metal blanks used in this study were perforated in the slot-type shape along the two curved bending lines of 200 mm radius, to facilitate easier bending of the material without macro- and microscopic induced defects [11]. The specific width, length and spacing from each adjacent slot are presented in Figure 3. The rectangular sheet metal blanks, the slot type perforations and the tensile samples were obtained by laser cutting process using Trumpf Trumatic L3020 Laser Cutting Machine with the following cutting parameters: nominal output power - 3,2 kW; gate frequency - 10 kHz; wavelength of the laser - 10.6 µm; duty cycle - 6.5%; scanning speed - 1.9 …5.9 m/min; nozzle gap - 1 mm; N_2 assisting gas pressure - 14 bar.

Further, the perforated rectangular blanks (Fig. 3) were submitted to the U-bending process along curved lines.

A customised bending tool was designed and modelled using SolidWorks software to analyse the behaviour of the EN AW-5754 aluminium alloy specimens during the cold U-bending process along curved lines. Bending tools (die and punch) were layer by layer 3D printed

through the Fused Deposition Modelling (FDM) technique from polymeric materials (ABS) using the Dimension 1200 3D printer. The U-bending process was conducted on a Trumpf TrumaBend V 1300 Press brake (F = 300 kN; Y-operating speed = 10 mm/s, punch stroke length= 55 mm).

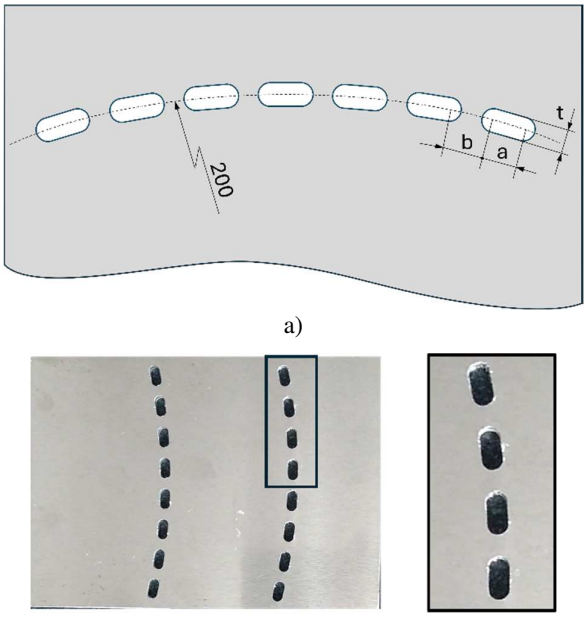

Fig. 3. The geometry and dimensions of the slots cut through metal sheet: a = 4 mm, b = 8 mm and t = 4 mm; (a) schematic representation; (b) perforated rectangular blank

The macroscopic characterisation of the U-bent specimens was carried out on specific samples using SMZ 745T Nikon stereo microscope. The metallographic analysis was performed on certain areas of interest of the U-bent specimens. Metallographic samples were cut using Struers Labotom 5 manual cut-off machine and then manually cold-mounted in acrylic resin and metallographically prepared for specific analyses. The grinding step was done using sandpapers of 220, 800, 1200 and 4000 grit sizes and the samples were then polished with 9 µm and 3 µm diamond suspension. Both grinding and polishing operations were performed on the automatic Struers Tegramin 25 machine. Polished samples were further etched with Keller's reagent (1 mL HCl, 1.5 mL HNO_3, 2.5 mL HF, and 95 mL H_2O) and light microscopy analysed by BX51M Olympus metallurgical microscope to investigate the cross-section morphology of the bent area. Also, these samples were examined by scanning electron microscopy (SEM) and elemental characterisation was performed by energy dispersive spectroscopy (EDS) analysis using Hitachi SEM SU8010 equipment operating at an accelerating voltage of 15 kV. Detailed information about the crystallographic structure and chemical composition was obtained through X-ray diffraction (XRD) analysis using the Rigaku SmartLab System.

3. RESULTS AND DISCUSSIONS

3.1 Mechanical properties

During the tensile tests, the experimental load versus displacement curves of EN AW 5754 aluminium alloy (Fig. 4) samples were obtained to determine the mechanical properties and behaviour of the material along RD-0°, TD-90° and DD-45° directions (see Fig. 2). The yield stresses, the ultimate tensile strengths, Young's moduli and the elongations after fracture of the investigated aluminium alloy in the three directions are summarised in Table 1.

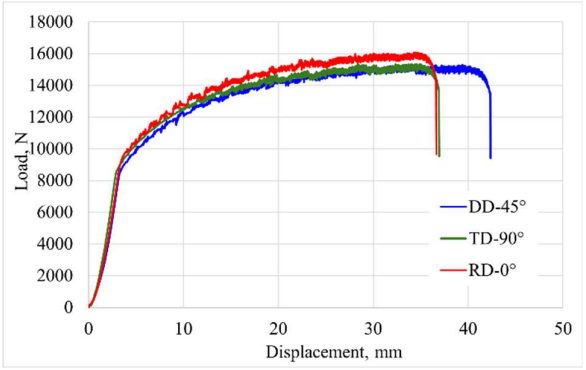

Fig. 4. Load versus displacement curves of EN AW-5754 samples in the rolling direction (RD-0°), transversal direction (TD-90°) and diagonal direction (DD-45°).

Table 1

Mechanical proprieties of EN AW-5457 aluminium alloy in three directions

	$Rp_{0,2}$ [MPa]	**R_m [MPa]**	**E [MPa]**	**A [%]**
RD-0	135,16	220,65	9864,9	17,25
TD-90	127,43	209,61	9916,16	19,14
OD-45	124,74	209,37	9685,5	20,68

It was found that regardless of the stress direction, Young's modulus is the same, which means that the stress is proportional to the strain,

that is, it obeys Hooke's law in the linear elastic region. In the strain-hardening and necking regions where the material becomes hardened and the local cross-sectional area becomes smaller leading to fracture, the rotation mechanisms of sliding systems specific to FCC metals occur [12]. For this reason, tensile strain values determined along the three specified directions are variable, there is a close relationship between the direction of the deformation and the number of sliding systems that come into action, one by one, as the tensile stress increases. This complex behaviour will be studied in a future paper dedicated to this purpose.

3.2 Microstructure

Optical microscopy

The parameters of the U-bend specimens used in this study are denoted as follows (Fig. 5):

- Convex CBL-o – outermost curved bending line on the convex side;
- Concave CBL-o – outermost curved bending line on the concave side;
- Convex CBL-i – innermost curved bending line on the convex side;
- Concave CBL-i – innermost curved bending line on the concave side;
- Ro - bending radius of the outermost fibres;
- Ri – bending radius of the innermost fibres;

The macroscopic investigation of the U-bent specimens with slot-type perforations processed along the two bending lines (Convex CBL and Concave CBL) revealed changes in the shape and size of the slots and the distance between the slots (Fig. 6 and Fig. 7). These changes occurred both on the inside and outside of the deformed zone, as the material undergoes tension on the outer fibre (Ro) and compression on the inner fibre (Ri).

The phenomena of the stretching of the outer fibres and the compression of the inner fibres were confirmed by the dimensional changes of the slots, before (Fig. 3) and after bending (Fig. 6 and Fig. 7). In the central area of the Convex CBL-o (Fig. 6c), the deformation of the perforated specimen resulted in an increase in slot length and width by approximately 13% and 105%, respectively, confirming that the outer fibres were under tension (Fig. 6c).

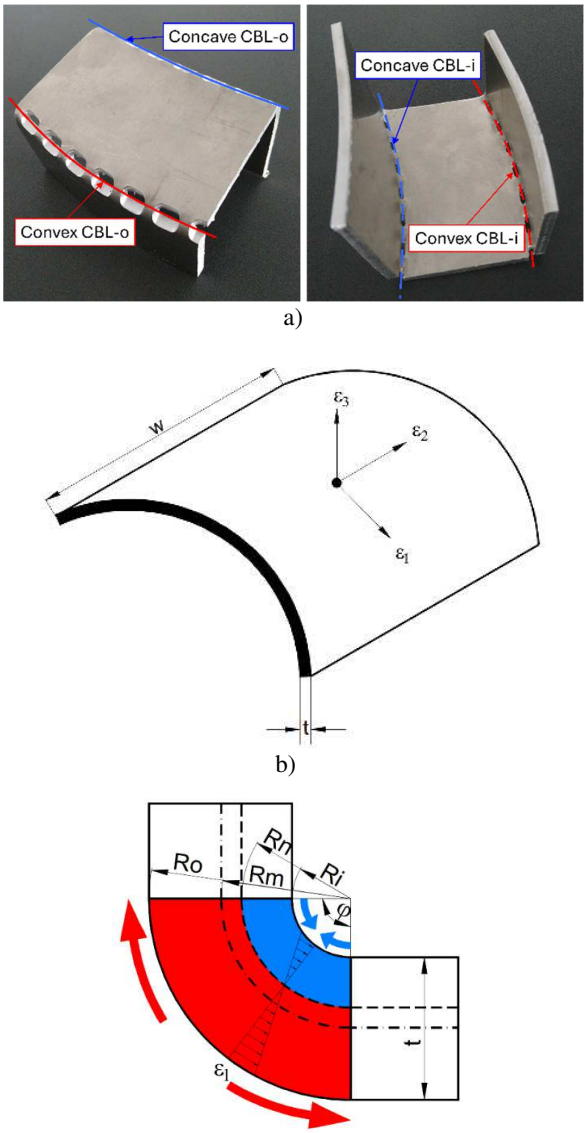

Fig. 5. EN AW-5754 specimens produced by the U-bending process along two perforated curved lines (a); strain state of the bent zone: ε_1, ε_2, ε_3 - the principal strains in the circumferential, transversal and radial direction (b); the distribution of compressed and stretched fibres across the sheet thickness t; Rm and Rn represent the median and neutral radii of the fibres (c)

In the marginal area of the Convex CBL-o (Fig. 6b), the slot length showed a similar variation (approx. 11%) as in the central area, but its width only increased by 70.5% compared to the unbent specimen. This indicates that the stretching of the fibres was maximum in the central area and decreased towards the marginal area of the Convex CBL-o. However, deviations from the regular shape of the slot were observed

in the marginal area, suggesting the need to identify an extrinsic cause of the material's behaviour. To address this, a comparison will be made between the central and marginal areas of the deformed slots.

In the case of the marginal slots (Fig. 6b and Fig. 7b), it was found that they had irregular shapes and smaller lengths and widths compared to the central slots (Fig. 6c and Fig. 7c). These morphological changes were due to the different behaviour of the material at the ends of the curved bending lines, where the circumferential and radial strain values were greater than those in the central area of the bending lines (see Fig. 5b). Thus, at the ends of the curved bending lines, the material experienced stronger contact with the surfaces of the bending tools and as a result, radial and circumferential strains increased due to a higher coefficient of friction [13].

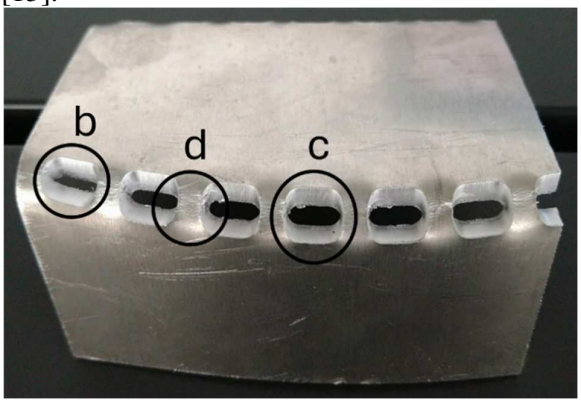

a)

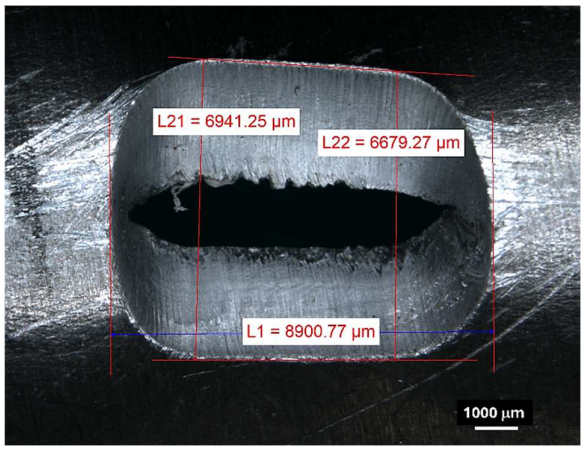

b)

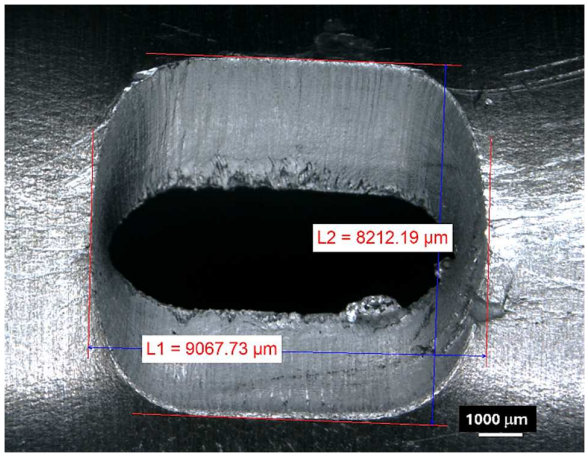

c)

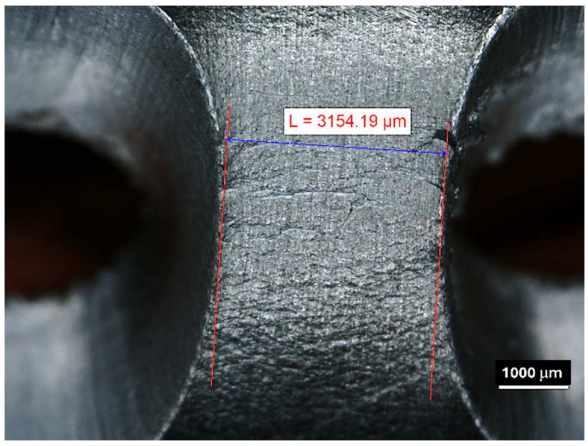

d)

Fig. 6. Macroscopic images of the slots: along the Convex CBL-o (a); shape and size of the slot near the edge (b) and in the centre of the bending line (c); distance between slots (d)

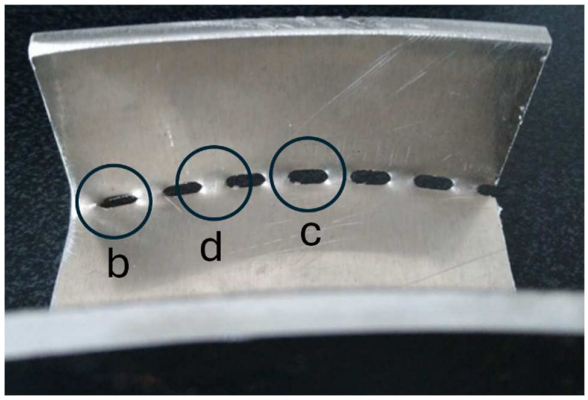

a)

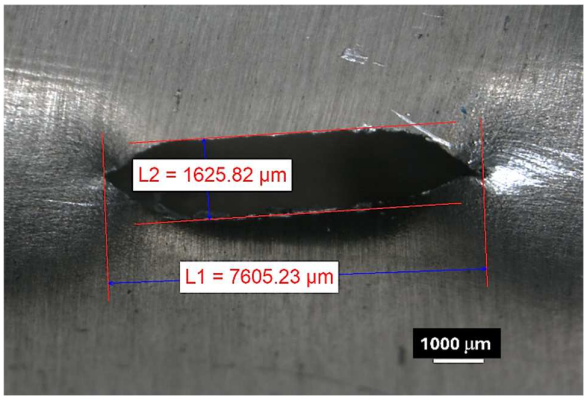

b)

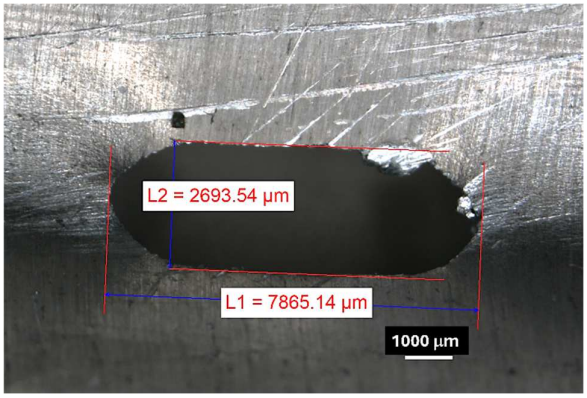

c)

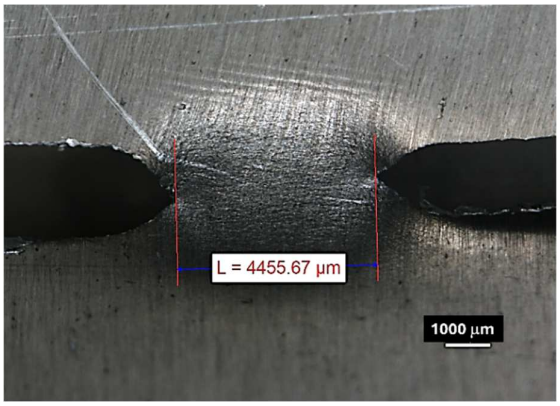

d)

Fig. 7. Macroscopic images of the slots: along the Convex CBL-i (a); shapes and size of the slot near the edge (b) and in the centre of the bending line (c); the distance between the slots (d)

Regarding the areas between the slots (Fig. 6d and Fig. 7d) both along the Concave CBL and the Convex CBL lines, the macroscopic investigation showed the formation of banded-type ridges and surface undulations. Zhang, Q., et all stated in their work [14] that these ridges and surface undulations were developed by the strain localisation of multiple layers of grains near the outer tensile surface. The initial roughness of the material surface was considered to favour the appearance of strain localisation, which led to important changes in the shape and orientation of the grains in the vicinity of the outer surface. These changes resulted in the formation of undulations and ridges on the outer tensile surface [15].

The microscopic characteristics of the samples in the plastic deformation areas validate the U-bending phenomena observed at the macroscopic level. The microstructure of the EN AW-5754 sheet shown in Figure 8 revealed structural homogeneity and texture and grain orientation according to the rolling direction.

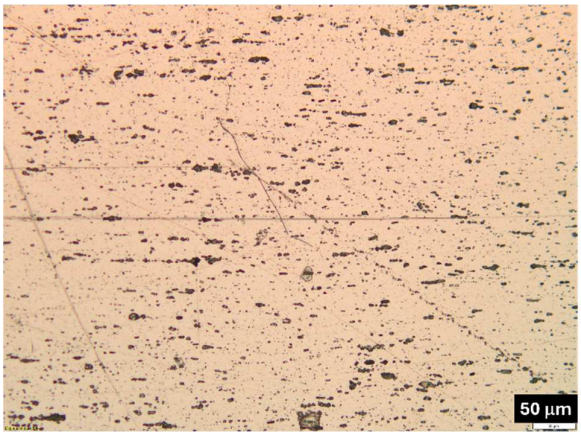

Fig. 8. Textured homogenous structure along the RD

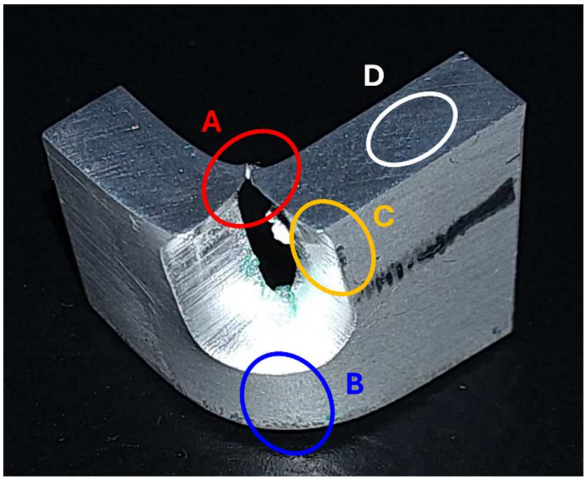

Fig. 9. Areas of interest with microstructural changes due to the U-bending process: **A** - cross-section through one of the ends of the slot on the inner side of the bending area (Ri, Fig. 5c); **B** - the area between the slots on the outer side of the bending area (Ro, Fig. 5c); **C** - cross-section through one of the ends of the slot on the outer side of the bending area (Ro, Fig. 5c); **D** - the area unaffected by the bending process

Figure 9 presents the areas of interest for microscopic analysis as they contain microstructural changes confirmed by recent research.

Figure 10a shows the macroscopic appearance of area **A** and Figure 10b represents the microscopic image of the yellow square detail.

At the microscopic level, microstructural changes in the crystalline grains were observed compared to the central area of the sample.

This is due to the compressive stresses that arose during the U-bending process and the strain-hardening specific to the cold plastic deformation process (Fig. 10c) [16, 17, 18].

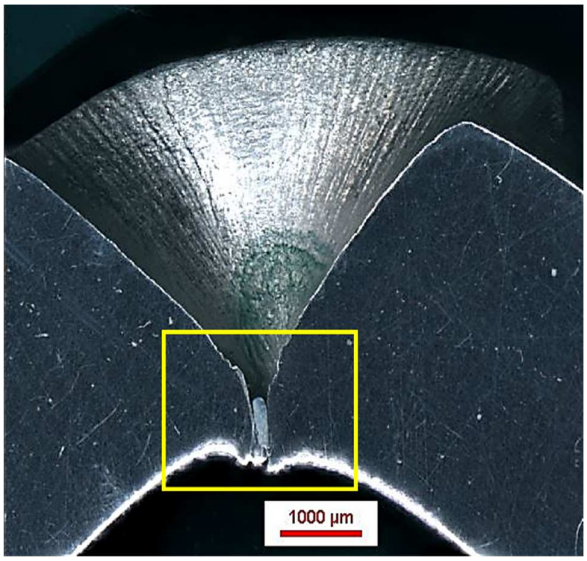

a)

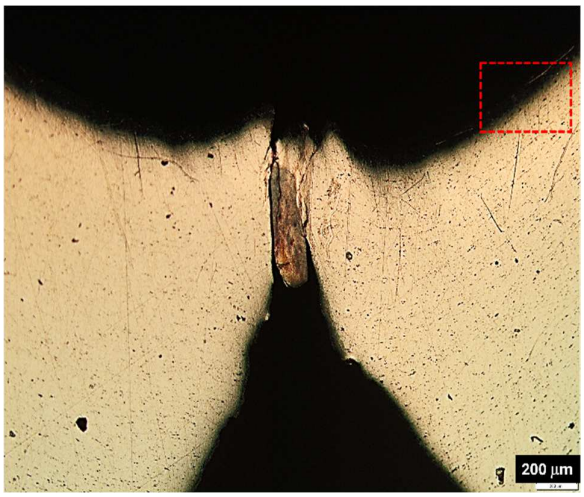

b)

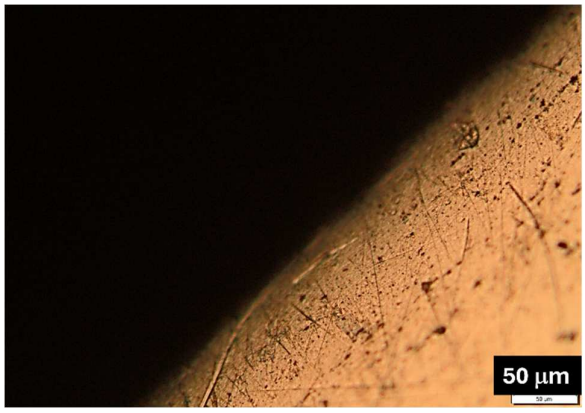

c)

Fig. 10. Morphological detail of zone **A**: a) macroscopic; b) microscopic localisation of the innermost fibres; c) strain-hardened layers

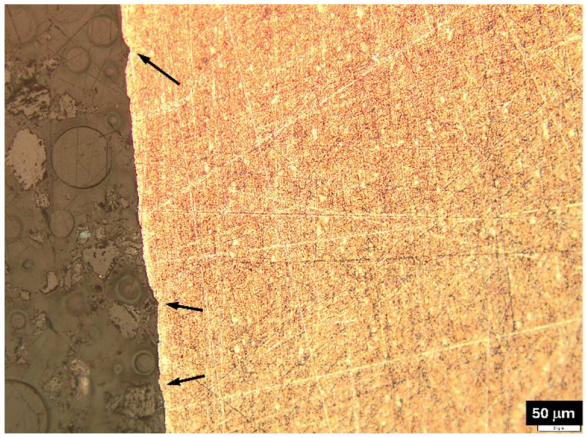

a)

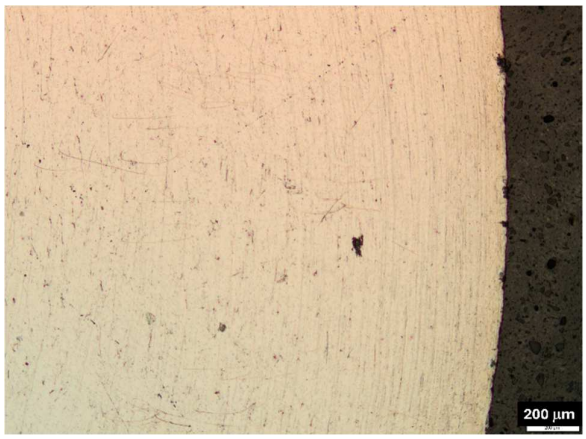

b)

Fig. 11. Microscopic image of the bending area **B** between the slots: a) surface undulations; b) multiple elongated fibres near the outer surface

Microscopic details of the area **B** are presented in Figure 11. As confirmed by other researchers [14, 15] and the macroscopic investigations given in the previous section,

surface undulations in the EN AW 5757 alloy (indicated by black arrows in Fig. 11a) were observed due to intense strain localisation of multiple layers of grains near the outer stretched surface (Fig. 11b).

The microscopic analysis of area **C** (Fig. 12a) shows a less intense stretching of the outer fibres due to the lack of material (perforated slot) so that only a few layers of material in the vicinity of the outer surface will deform.

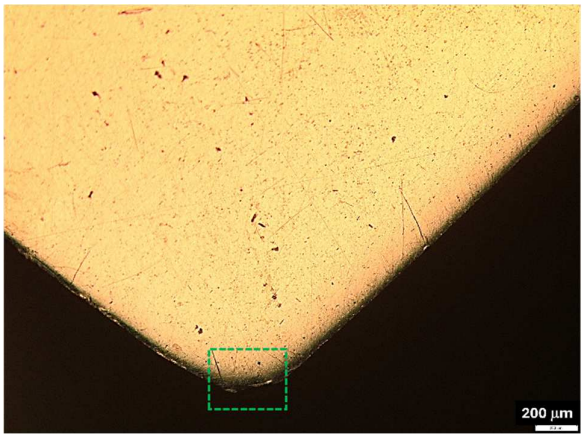

a)

b)

Fig. 12. Microscopic images of **C** zone (a) and green square detail with few banded-type ridges near the outer surface (b)

Electronic microscopy

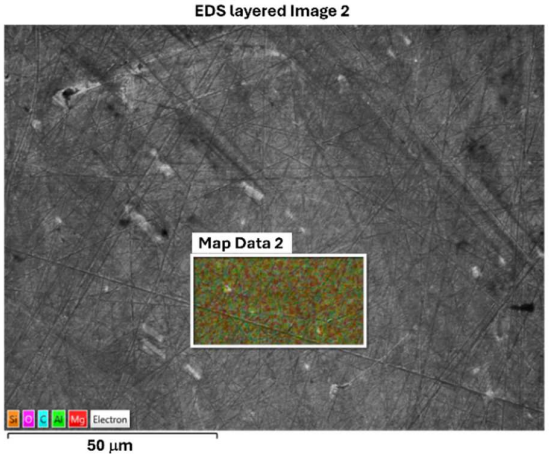

a)

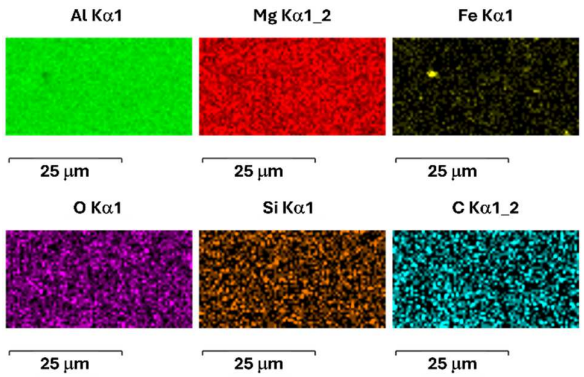

b)

Fig.13. SEM (a) and EDS (b) tests on the sheet metal blank

X-ray diffraction analysis

X-ray diffraction (Fig. 14) was performed in 3 different areas (see Fig. 9): **B** - bending area; **C** - slot area; **D** – area unaffected by the bending process. The purpose of the analysis in these 3 areas was to identify the state of residual stresses after the U-bending process.

The diffraction maxima were identified as aluminium (the main chemical element of the sample material) according to the ICDD database, with card number 001-1176. From the angular position values of the diffraction maxima, it is evident that there are no changes in the interplanar spacing, and therefore, in the lattice constant from one area to another. Consequently, the bending process did not induce stress states with a potential negative impact on the functionality of the dynamic façade module which will be further researched.

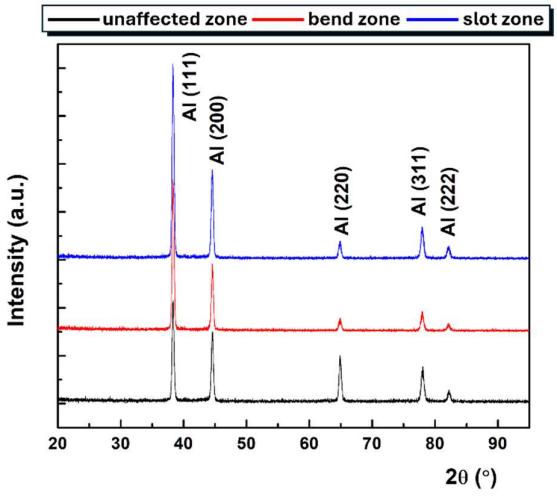

Fig. 14. XRD patterns for the studied samples in the specified areas

4. CONCLUSIONS

The study highlighted the importance of understanding the structural aspects that can arise during the cold-forming processes of the modular elements of the dynamic facades made from EN AW 5754. The following conclusions can be drawn:

- the specimen is mechanically isotropic in its rolled state, which is confirmed by the results of tensile testing in different directions relative to the rolling direction;
- at the macrostructural level, the U-bending process determined the outer fibres to stretch and the inner fibres to compress, affecting the morphology of the specimens in the bending zone;
- at the microscopic level, the crystalline structure of the material confirms the phenomena of stretching and compression through microstructural changes generated by the strain localisation of layers in the analysed areas;
- perforated slots contribute to improved U-bending behaviour of specimen material;
- the U-bending process did not adversely affect the residual stress state in the structure of the specimens, which could be advantageous for the functionality of the facade modules. This aspect will be further investigated.

5. ACKNOWLEDGEMENT

This work was supported by the Project PN-III-P2-2.1-PED-2019-4624 / nr. 468/23.10.2020, Spatial structures designed for complex, lightweight structures processed by Curved Crease Folding (CCF-Surf).

6. REFERENCES

[1] Aelenei, D., Aelenei L., Pacheco, V. C., *Adaptive Façade: concept, applications, research questions,* Energy Procedia 91, pp. 269 – 275, 2016.

[2] Loonen, R.C.G.M., Trčka, M., Cóstola, D., Hensen J.L.M, *Climate adaptive building shells: State-of-the-art and future challenges,* Renewable and Sustainable Energy Reviews 25, pp. 483–493, 2013.

[3] Gonçalves M., Figueiredo, A., Almeida, R.M.S.F., R. Vicente, *Dynamic façades in buildings: A systematic review across thermal comfort, energy efficiency and daylight performance*, Renewable and Sustainable Energy Reviews 199, pp. 114474, 2024.

[4] Sommese, F, Badarnah, L, Ausiello, G., *A critical review of biomimetic building envelopes: towards a bio-adaptive model from nature to architecture*. Renewable and Sustainable Energy Reviews 169, pp. 112850, 2022.

[5] Sommese, F., Badarnah, L., Ausiello, G., *Smart materials for biomimetic building envelopes: current trends and potential applications*. Renewable and Sustainable Energy Reviews 188, pp. 113847, 2023.

[6] Snopiński, P., Tański, T., Gołombek, K., Rusz, S., Hilser, O., Donič, T., Nuckowski, P. M., Benedyk, M., *Strengthening of AA5754 Aluminum Alloy by DRECE Process Followed by Annealing Response Investigation*, Materials 13, pp. 301, 2020.

[7] Waqas, M., Jidong, K., Abhijit, P. B., Usman, A., Jürgen, H., Henk-Jan B., Olaf, E., Raja, M., Kaan, I., *Bendability enhancement of an age-hardenable aluminum alloy: Part I — relationship between microstructure, plastic deformation and fracture*, Materials Science & Engineering A 753, pp. 179–191, 2019.

[8] Sarkar J., Kutty T.R.G., Conlon K.T., Wilkinson D.S, Embury J.D., *Tensile and bending properties of AA5754 aluminum alloys*, Materials Science and Engineering A316, pp. 52–59, 2001.

[9] Mucha, J., Kaščák, L'., Witkowski, W., *Research on the Influence of the AW 5754 Aluminum Alloy State Condition and Sheet Arrangements with AW 6082 Aluminum Alloy on the Forming Process and Strength of the ClinchRivet Joints*, Materials 14, pp. 2980. 2021.

[10] Yan, Z., Xiao, A., Zhao, P., Cui, X., Yu, H., Lin, Y., *Deformation behavior of 5052 aluminum alloy sheets during electromagnetic hydraulic forming*, Int, J. of

Machine Tools & Manufacture 179 pp. 103916, 2022.
[11] US Patent No US 6,640,605 B2, *Method of bending sheet metal to form three-dimensional structures*, Nov. 4, 2003.
[12] Wang, R., Lu C., Tieu, K.A., Gazder, A.G., *Slip system activity and lattice rotation in polycrystalline copper during uniaxial tension,* Journal of materials research and Technology, 18, pp. 508-519, 2022.
[13] Dewang, Y., Hora, M.S., Panthi, S.K., *Effect of process parameters on deformation behavior of AA 5052 sheets in stretch flanging process*, Materials Today: Proceedings 4, pp. 9316–9326, 2017.
[14] Zhang, Q., Xu, X., Wang, Y., *Effect of Mg/Si Ratio on the Bendability and Anisotropic Bend Behavior of Extruded 6000-Series Al Alloy*, Materials 16, pp. 3599, 2023.
[15] Mattei, L., Daniel, D, Guiglionda, G., Klocker, H., Driver, J., *Strain localization and damage mechanisms during bending of AA6016 sheet*, Materials Science & Engineering A559, pp. 812–821, 2013.
[16] Raabe, D., *Recovery and Recrystallization: Phenomena, Physics, Models, Simulation*, In Physical Metallurgy, Fifth Edition, pp. 2291-2397, 2015, Elsevier.
[17] Sakai, T., Belyakov, A., Kaibyshev, R., Miura, H., Jonas, J.J., *Dynamic and post-dynamic recrystallization under hot, cold and severe plastic deformation conditions*, Progress in Materials Science 60, pp. 130–207, 2014.
[18] Hamed, A., Rayaprolu, S., Winther, G., Anter El-Azab, A., *Impact of the plastic deformation microstructure in metals on the kinetics of recrystallization: A phase-field study*, Acta Materialia 240, pp. 118332, 2022.

Analiza structurala a elementelor modulare pentru fatade dinamice realizate prin tehnologia de indoire in U

Aliajul de aluminiu EN AW-5754 prezintă un interes deosebit pentru proiectanții din domeniul fațadelor inteligente de clădiri, fiind capabil de ajustări arhitecturale cinematice și dinamice în funcție de condițiile climatice excesive de funcționare (temperatură, luminozitate, curent de aer). Studiul își propune să realizeze o analiză structurală complexă a modulelor de fațadă din aliajul EN AW-5754, fabricate prin tehnologia de indoire în U. Pentru a facilita deplasarea volumetrica a materialului in timpul deformarii plastice, respectiv pentru a evita defectele structurale specifice, modulele de fatada sunt perforate cu precizie de-a lungul curbelor de indoire; pentru acest scop, tehnologia cu fascicul laser permite realizarea de diferite modele personalizate de perforatii. Rezultatele analizei evidențiază influența perforatiilor personalizate asupra calității suprafeței elementelor modulare in zonele de îndoire.

Cristina TEISANU, PhD, Assoc. Prof., University of Craiova, Faculty of Mechanics, Department of Automotive Transportation and Industrial Engineering, cristina.teisanu@edu.ucv.ro, 107, Calea Bucuresti, Craiova, Romania.
Nicoleta CIOATERA, PhD, Assoc. Prof., University of Craiova, Faculty of Sciences, Department of Chemistry, nicoleta.cioatera@edu.ucv.ro, 107, Calea Bucuresti, Craiova, Romania.
Leonard Marius CIUREZU-GHERGHE, PhD, Lecturer, **corresponding author**, University of Craiova, Faculty of Mechanics, Department of Automotive Transportation and Industrial Engineering, leonard.ciurezu@edu.ucv.ro, 107, Calea Bucuresti, Craiova, Romania.
Gabriela SIMA, PhD, Assoc. Prof., University of Craiova, Faculty of Mechanics, Department of Engineering and Management of Technological Systems, gabriela.sima@edu.ucv.ro, 1, Calugareni, Drobeta Turnu Severin, Romania.
Cristian CHIHAIA, PhD student, University of Craiova, Faculty of Mechanics, c.cristian.cde@gmail.com,107, Calea Bucuresti, Craiova, Romania,
Cosmin MIRITOIU, PhD, Assoc. Prof., University of Craiova, Faculty of Mechanics, Department of Applied Mechanics and Civil Engineering, cosmin.miritoiu@edu.ucv.ro, 107, Calea Bucuresti, Craiova, Romania.